# Experimental and Theoretical Analysis of Ink Dispersion Stability for Polymer Electrolyte Fuel Cell Applications

S. Shukla,[a] S. Bhattacharjee,[a,c] A. Z. Weber,[b,*] and M. Secanell[a,*,z]

[a]*Department of Mechanical Engineering, University of Alberta, Edmonton, AB, Canada*
[b]*Energy Conversion Group, Lawrence Berkeley National Laboratory, Berkeley, California 94720, USA*

The aggregate size in fuel cell catalyst inks depends on the type of dispersion medium, particle concentration, and addition of stabilizing agents. In this work, ink stability and particle size of carbon black and carbon black/Nafion dispersions in four non-aqueous media, viz., methanol, ethanol, isopropanol and ethyl acetate are studied. Based on visual inspection, isopropanol is found to be the best medium for dispersion of carbon black inks. To rationalize this observation, a semi-empirical model based on diffusion-limited aggregation was developed to evaluate the rate of particle aggregation and predict the ink stability time for each dispersion medium. The proposed model supports the experimental observation by qualitatively predicting the same relationship between carbon stability and the dispersion media. The model also showed that the dielectric constant of the dispersion medium and the particle zeta potential are primarily responsible for the ink stability. Particle size for the different inks was determined by dynamic light scattering with and without dilution. Experimental results show that Nafion is a strong stabilizing agent, increasing the ink stability and decreasing the particle size of carbon aggregates. The beneficial effects of Nafion are independent of its concentration and are observed even at Nafion volume fractions of 10 wt%. The interaction energy is found to be a strong function of the surface potential for the dispersion medium with a higher dielectric constant.

Most catalyst layer (CL) fabrication methods for polymer-electrolyte fuel cells (PEFCs) to date are based on wet deposition of a colloidal dispersion, i.e., the catalyst ink, onto either a membrane or a diffusion medium.[1,2] The CL ink is usually a mixture of carbon-supported platinum particles, ionomer and a dispersion medium (DM). Ink stability, defined as the ability of particles to remain dispersed in the DM, and a reduced aggregate size are critical to deposition methods such as inkjet printing[3–6] and spray coating.[1,7,8] Inkjet printing allows for controlled spacial resolution,[6] however in order to create appropriate droplet sizes, the ink has to be ejected from micrometer size nozzles,[5] easily resulting in nozzle clogging. Inkjet printing of microporous layers using carbon ink has also been found to be extremely difficult unless ionomer solution, acting as a stabilizing agent, is added to the ink.[9] Similarly, spray coating requires inks to go through a nozzle, therefore clogging issues are likely to be a challenge when small nozzle sizes are used. Control over the aggregate size and the right selection of a DM to achieve the desired viscosity and surface tension therefore becomes critical in these deposition techniques. Further, the ink stability may also be important to larger commercial fabrication processes to increase the ink storage time.

Even though the importance of appropriate ink recipes has been recognized,[1,10] very few studies have aimed at understanding the impact of DM on the ink stability. The type of DM, particle concentration and the ink's ionomer content will dictate its stability and aggregate size. This, in turn, will dictate the viscosity and surface tension of the ink, and ultimately, performance of the electrode since it governs the CL microstructure.[1,11] Poor Pt utilization occurs due to transport losses taking place at the macro and micro-scale of the CL.[12,13] The micro-scale transport depends on the aggregate structure and ionomer distribution in the CL. The transport losses at this scale become important especially for low Pt loading electrodes where the micro-scale transport resistance is predominant due to the higher local volumetric current density.[4,14–17]

The type of DM affects the structure of the ionomer dispersed in it.[18–21] Ink properties are also affected by the DM as observed in a number of studies comparing the electrochemical performances of electrodes with the same ink components but different DM.[11,21–25] Shin et al.[11] concluded that the electrodes fabricated using a n-butyl acetate based ink had a higher electrochemical surface area and performed better as compared to an IPA based ink. Millington et al.[25] found that using tetrahydrofuran in the ink improved the CL performance, whereas using ethylene glycol and glycerol led to poor performances. Malek et al.[26] and Xiao et al.[27] used coarse-grained molecular-dynamics (CGMD) simulations to study the interaction of carbon, Nafion and the DM. Malek[26] reported an increasing agglomerate size with decreasing dielectric constant of the DM which was validated experimentally by measuring the catalyst particle size in a range of DM. Although the model predictions for the aggregate size varied quantitatively, the qualitative assessment was confirmed.[26]

In spite of being one of the major factors in the ink preparation process, the DM selection is done either by a simplistic empirical approach or by using complex molecular-dynamics simulations. A simple semi-empirical model to predict the differences in particle-particle interactions and ink stability with changing DM would be useful to determine the "goodness" of a particular dispersion medium. In this work, a modified form of the Derjaguin-Landau-Verwey-Overbeek (DLVO) model is implemented to determine the interaction energy between the colloidal particles and subsequently the stability ratio for different non-aqueous DM. Quantification of settling time for the aggregates in the ink is carried out based on a population balance assuming a diffusion-limited aggregation process. Experimental validation using carbon based inks in isopropanol (IPA), ethyl acetate, ethanol and methanol is done using transient stability tests based on visual inspection and dynamic light scattering (DLS) to determine the particle size. Further, part of the DLS study is carried out without diluting the ink sample, thus revealing a more accurate particle size. It is believed that this work may serve as a foundation upon which more complex physics of particle interactions, such as the effect of ionomer chains (steric interactions), can be implemented. In addition to ink stability, a CL ink should also be easy to coat on the substrate and not de-wet. Coatability and wettability are governed by viscosity, evaporation rate and surface tension. These parameters will not be discussed in this article even though they are equally important. Also, the present work does not take into account the extent of reversibility of the aggregation process, where applying an external shear force may break the aggregates and re-disperse the particles.

The paper is organized in the following way. The experimental section provides information about the materials used for ink fabrication, ink preparation process and size analysis. The theory section gives an overview of the model developed. The results section discusses the

---

*Electrochemical Society Member.
[c]Present address: Water Planet Engineering, Inglewood, CA 90301, USA.
[z]E-mail: secanell@ualberta.ca

effect of the DM on the ink stability, the effect of Nafion and dilution on ink particle size.

## Experimental

***Sample preparation.***—Experiments were carried out using non-aqueous DM, i.e., IPA ($\geq$ 99.5% Sigma Aldrich), ethyl acetate (HPLC grade, Fisher Scientific), methanol (HPLC grade, Fisher Scientific) and ethanol (Commercial Alcohols Inc.). They were chosen because of the difference in their dielectric constants, a property which dictates particle interaction, available literature data for zeta potential of carbon black in these media, and their common use in catalyst ink preparation.[7,28] Commercially available carbon black, Vulcan XC-72R (Fuel Cell Store) was used as received. The standard operating protocol used for the ink preparation was similar to that used in our previous work.[29] The inks were prepared in glass vials by mixing 12.5 mg of carbon black with 3.5 mL of the DM. The Nafion solution contained 5 wt% Nafion ionomer, 45 $\pm$ 3 wt% water and volatile organic compounds as the rest. When adding Nafion, the volume of DM was adjusted in order to maintain a constant solid fraction. The amount of ionomer to be added to the ink was calculated using the following relation[4]

$$Y_{el} = \frac{m_N}{m_N + m_C} \times 100 \qquad [1]$$

where $Y_{el}$ is the weight % of the ionomer to be added, $m_N$ is the mass of Nafion and $m_C$ is the mass of carbon.

The dispersion was mixed using a sonication bath (Branson 1800) for at least 45 minutes. When considering the effect of Nafion, the ionomer solution was added drop-wise to the dispersion. It was further mixed with a probe sonicator (QSonica S-4000) at an amplitude of 20% for 15 minutes (2 min. ON and 1 min. OFF) to break up the aggregates and homogenize the suspension (this step was excluded for the inks when measuring the cumulants diameter using light scattering at Lawrence Berkeley National Laboratory). The sample was finally stirred using a magnetic stirrer for 10 minutes before leaving it undisturbed for further testing.

***Particle size analysis.***—Dynamic light scattering (DLS) was employed to determine the hydrodynamic diameter of the particles in the ink using ALV/CGS-3 Compact Goniometer System. Another DLS system at Lawrence Berkeley National Laboratory (Micromeritics NanoPlus 3) was also used to analyze the average (cumulants) diameter in the inks, since it allowed for direct measurement of the sample without dilution. When involving dilution, the sample was prepared by mixing the ink with the respective DM to less than 1% (or a specified amount) of its original weight. Prior to testing, the sample was allowed to equilibrate to 25°C. The scattering angle was kept at 90°. The input parameters, viscosity and refractive index of the DM used for IPA were 1.96 cP/1.374, for ethyl acetate were 0.426 cP/1.372, for methanol were 0.554 cP/1.326 and for ethanol were 1.09 cP/1.361 respectively. For carbon black, the real part of its refractive index at a wavelength of 1.75 $\mu$m, i.e., 2.47, was taken.[30,31] The attenuation coefficient at this wavelength is negligibly small, thus the imaginary component of the refractive index can be neglected here. For each sample, a minimum of three runs were conducted with a time of at least 660 sec/run and a gap of at least 2 minutes between each run.

It should be noted that DLS results are highly sensitive to the presence of larger aggregates that may lead to an overestimation of particle size.[32] Further, the particle size obtained from DLS is either the hydrodynamic diameter (ALV/CGS-3) or the cumulants diameter (NanoPlus 3) for non-spherical particles and this value may be greater if the particle surface consists of attached polymer chains. These drawbacks mean that DLS results can only be used for a qualitative assessment of particle size.

***Mercury intrusion porosimetry.***—The density of Vulcan XC-72 carbon black was evaluated by using mercury intrusion porosimetry (Poremaster 33, Quantachrome Instruments). Details regarding the

experimental procedure have been described in our previous work.[5] The averaged true density value of carbon black, $\rho_p$, was found to be 1.69 $\pm$ 0.21 g/cm$^3$ based on 4 independent tests using an intrusion pressure of up to 33,000 psi.

## Theory

A catalyst ink can be considered as a colloidal dispersion of particles in a liquid medium. When introduced in a DM, these nanoparticles will tend to collide with each other due to their random Brownian motion. If the collision energies are large enough to overcome the repulsive energy barrier, they will lead to the formation of aggregates.[33] These aggregates will increase in size and at a point when the aggregate size can no longer remain in a state of colloidal dispersion, sedimentation will take place resulting in a non-dispersed ink. In order to prevent this phase separation and keep the aggregate size as small as possible, a suitable DM needs to be selected and the interacting energies acting on the nanoparticles need to be studied. This section describes the evaluation of parameters used in the semi-empirical model for ink stability.

***Assumptions.***—The following assumptions are used for the model:

• Carbon particles are idealized as being perfectly spherical with a diameter of 25 nm,[34] suspended in infinitely dilute concentrations in the DM at room temperature.
• Particle collisions are purely diffusion-limited, i.e., perikinetic aggregation.
• Screening effects are absent in non-aqueous DM and the repulsive force is provided by Coulombic interactions.
• The zeta potential, $\zeta$, is assumed to be equal to the particle surface potential, $\psi$.

***Evaluation of interaction energy (U).***—Figure 1 shows the interacting energies between two colloidal particles of radius $a$ separated by a distance $h$ suspended in a DM. The distance between the center of the two particles is represented by $r$. The main interaction energies acting on the particles include attractive van der Waals (vdW) (arising from dipole-dipole interactions), repulsive Coulombic/electrostatic energies (arising from surface potential and electric double layer), steric interactions (caused by an attached polymer chain) as well as other forces such as hydrophobic interaction and drag.[35]

For the case of aqueous dispersion, the particle surface potential ($\zeta$) will attract counter-ions from the DM around the particle to form an electric double-layer, as shown in Figure 1. These electric double layers provide electrostatic repulsion when they interact as the particles approach. For the case of non-aqueous dispersion when counter-ion concentration is very low or absent, Coulombic interaction replaces the electrostatic double layer interaction between the particles.[36] The attractive energy between the particles is in the form of van der Waals interaction.

When $a >> h$ (*Derjaguin* approximation), the van der Waals expression for two interacting spherical particles of radius $a_i$ and $a_j$ takes the form[37]

$$U_{vdW} = -\frac{A}{6} \cdot \left( \frac{a_i a_j}{a_i + a_j} \right) \cdot \frac{1}{r - (a_i + a_j)} \qquad [2]$$

where $U_{vdW}$ is the interacting energy, $A$ is the Hamaker constant and the negative sign indicates attractive interaction. The Hamaker constant ($A$) is a function of the particle and medium dielectric and optical properties and is approximated as,[35]

$$A = \frac{3}{4} k_B T \left( \frac{\epsilon_p - \epsilon_m}{\epsilon_p + \epsilon_m} \right)^2 + \frac{3 h \nu_e}{16\sqrt{2}} \frac{(n_p^2 - n_m^2)^2}{(n_p^2 + n_m^2)^{3/2}} \qquad [3]$$

where $\epsilon_p$ is the particle dielectric constant and $\epsilon_m$ is the medium dielectric constant. $n_p$ and $n_m$ are the respective refractive indexes for particle and medium. The constant used for absorption frequency $\nu_e$ is taken as $5 \times 10^{15} s^{-1}$.[35]
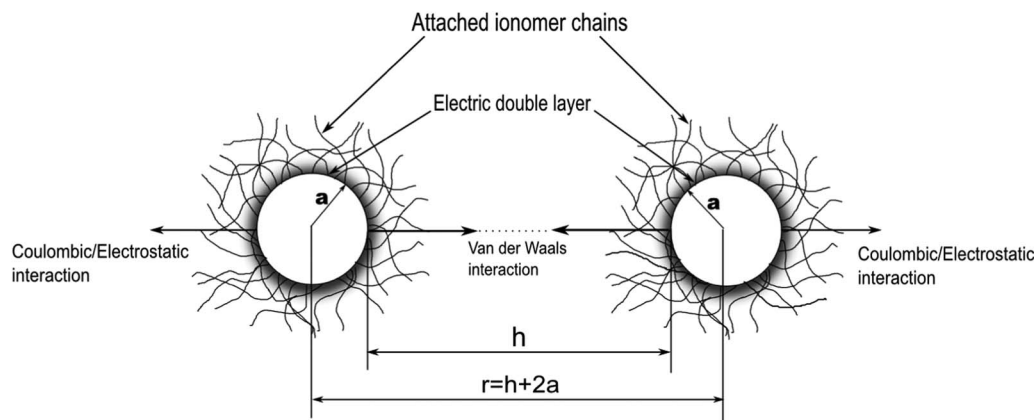
**Figure 1.** Interactions between the colloidal particles when suspended in a liquid medium showing the van der Waals, electrostatic and Coulombic interactions.

The repulsive Coulombic interaction ($U_{cf}$) takes the form[38]

$$U_{cf} = \frac{4\pi\epsilon_m^* \psi^2 (a_i + a_j)^2}{r} \quad [4]$$

where $\psi$ is the particle surface potential and $\epsilon_m^*$ is the absolute permittivity of the medium. The overall energy balance for the two particles is written as the sum of the van der Waals and Coulombic energies. Thus, the total interaction energy ($U_{tot}$) becomes,

$$U_{tot}(r) = U_{vdw} + U_{cf} \quad [5]$$

Equation 5 is a modified form of the commonly known DLVO type particle interaction.

*Aggregation kinetics.*—During the aggregation process, two primary particles (monomers) collide and aggregate to form a dimer, while a monomer and a dimer collide to form a trimer, which is an aggregate of three primary particles. Considering diffusion-limited (perikinetic) aggregation, the population-balance equation gives the rate of change of particle number concentration, i.e., number of particles per unit volume of ink with time.[33] Considering that particles $i$ and $j$ collide to form particle $k$, the concentration of particle $k$ can be written as[33]

$$\frac{dn_k}{dt} = \frac{K_{ij}}{2} \sum_{i=1; j=k-i}^{i=k-1} n_i n_j - K_{ik} n_k \sum_{i=1}^{\infty} n_i \quad [6]$$

where $n_i$, $n_j$ and $n_k$ represent concentration of $i$, $j$ and $k$ particle aggregates respectively and $K_{ij}$ is the rate constant of aggregation. For two colliding particles of radius $a_i$ and $a_j$, the collision rate constant, $K_{ij}$ is given as[33]

$$K_{ij} = \frac{2k_B T}{3\mu} \frac{(a_i + a_j)^2}{a_i a_j} \quad [7]$$

where $k_B T$ is the thermal energy associated with the particles and $\mu$ is the DM viscosity.

Equation 6 allows the possibility to plot the rate of decay of particle number-concentration with time, for a given particle size. These equations assume a collision efficiency of unity i.e., all collisions lead to aggregate formation. However, the collision efficiency ($\alpha$) will depend upon the particle interactions and change with the type of DM. A DM in which repulsive energy between the colloidal particles is greater than the attractive energy will have a lower collision efficiency since not all collisions will lead to the formation of aggregates.[33] Thus, including the collision efficiency, Equations 6 becomes,

$$\frac{dn_k}{dt} = \alpha \left( \frac{K_{ij}}{2} \sum_{i=1; j=k-i}^{i=k-1} n_i n_j - K_{ik} n_k \sum_{i=1}^{\infty} n_i \right) \quad [8]$$

The collision efficiency, $\alpha$, is the inverse of the stability ratio, $W$. The stability ratio is defined as the ratio of collision rate in the absence of any external forces, i.e., solely due to Brownian motion, to the collision rate considering inter-particle interactions, and is given as[39]

$$W = \frac{1}{\alpha} = (a_i + a_j) \int_{(a_i + a_j + a_t)}^{\infty} \frac{1}{r^2} exp\left( \frac{U_{tot}(r)}{k_B T} \right) dr \quad [9]$$

where $U_{tot}(r)$ is the total inter-particle interaction given by Equation 5. The value of $W$ was calculated by numerically integrating the expression in MATLAB. A minimum cutoff distance of 0.5 nm ($a_t$) was added while evaluating $W$ in order to prevent the inter-particle distance from reaching zero (i.e., finite size effects).

*Sedimentation-diffusion equilibrium.*—Given the hydrodynamic particle diameter, it is possible to plot the particle number-density, $n$, with respect to the height, $z$, of the colloidal suspension by using the sedimentation-diffusion equilibrium equation.[38] This relation makes use of the particle terminal velocity and Stefan velocity, which is the diffusive flux expressed in the form of a linear velocity. At equilibrium, the Stefan velocity is equal to the hindered terminal settling velocity,[37]

$$-D\frac{dln\, n}{dz} = \frac{4a^2(\rho_e - \rho)g}{18\mu}(1 - \phi_p)^{4.6} \quad [10]$$

where $a$ is the hydrodynamic radius of the particle aggregates, $\rho_e$ is the carbon aggregate effective density, $\rho$ is the DM density, $\mu$ is the DM viscosity, $g$ is the acceleration due to gravity (9.81 m/s²) and $\phi_p$ is the solid volume fraction in the DM. The value of $\phi_p$ is found to be 0.0021, thus justifying the assumption of an infinitely dilute concentration. The particle effective density, $\rho_e$, accounts for the density variation due to the entrained liquid in the aggregate pores, and is estimated using the following relation,[40]

$$\rho_e = \rho P + (1 - P)\rho_p \quad [11]$$

where $P$ is the inter-particle porosity for the Vulcan carbon aggregates. Based on a true primary carbon particle density of 1.69 g/cm³ and an inter-particle porosity of 0.676,[41] the effective density was found to be 1.08 g/cm³. The variation of $\rho_e$ with DM was found to be minimal, owing to the similar value of densities for the DM considered.

Solving for the condition that $n(z = 0) = n_0$ and recalling Einstein's relation

$$D = \frac{k_B T}{6\pi\mu a} \quad [12]$$

**Table I. List of constants and parameters used for the four dispersion media.**

| Dispersion Media | Dielectric constant, $\epsilon$ | Zeta Potential of CB in media, $\zeta$ (mV) | Refractive Index, $n$ | Hamaker constant, $A$ (J) |
|---|---|---|---|---|
| Ethyl Acetate | 6.0 | −50.0 | 1.37 | $3.48 \times 10^{-19}$ |
| Isopropanol | 18.0 | −71.1[28] | 1.37 | $3.49 \times 10^{-19}$ |
| Methanol | 33.0 | −28.5[28] | 1.33 | $3.75 \times 10^{-19}$ |
| Ethanol | 25.3 | −44.9[28] | 1.36 | $3.55 \times 10^{-19}$ |

the particle concentration distribution for any given aggregate radius, $a$, is

$$n(z) = n_0 exp \left[ \frac{-\pi 8 a^3 (\rho_e - \rho) g (1 - \phi_p)^{4.6}}{6 k_B T} z \right] \quad [13]$$

Using this relation, a plot of particle number-density profile with height can be obtained.

***Input parameters.***—Constants used for the DM and particles are given in Table I. The values of zeta potential for carbon black in IPA, methanol and ethanol were obtained from literature.[28] A value of $\zeta$ for carbon black in ethyl acetate was not found. Hence, a potential of −50 mV was considered here. Performing a sensitivity analysis, it was found that the ink stability was not a strong function of zeta potential for the case of ethyl acetate. Hence an approximate value of potential can be valid here. This has been discussed further in Effect of Nafion section.

To determine the size of an aggregate of $i$ monomers, its radius, $a_i$, is expressed as,

$$a_i = \left( \frac{a_p^3 i}{1 - P} \right)^{1/3} \quad [14]$$

where $a_p$ is the radius of primary carbon particle and $P$ is the interparticle porosity. Determining the time required for a particle to reach the threshold size, i.e., size beyond which sedimentation occurs, based on Equation 8 was computationally time consuming. Therefore, the stability time needed to reach a threshold aggregate size was estimated assuming monodispersed particle sizes. If equal particle radii are considered ($a_i = a_j$), which is a reasonable assumption only during early stages of aggregation,[33] the value of $K$ becomes independent of the particle size,

$$K = \frac{8 k_B T}{3 \mu} \quad [15]$$

and the population balance equation can be written as,[33,37]

$$\frac{dn_t}{dt} = -\alpha \frac{K}{2} n_t^2 \quad [16]$$

**Table II. Effect of particle size on Stability Ratio ($W$) for carbon black in ethyl acetate, methanol, ethanol and IPA.**

| Particle diameter (nm) | Ethyl Acetate | Methanol | Ethanol | Isopropanol |
|---|---|---|---|---|
| 25 | 0.29 | 0.40 | 1.29 | 19.69 |
| 30 | 0.32 | 0.49 | 2.33 | 89.60 |
| 60 | 0.64 | 2.46 | 278.52 | $6.03 \times 10^{6}$ |
| 90 | 1.59 | 23.77 | $1.26 \times 10^{5}$ | $2.36 \times 10^{12}$ |
| 120 | 4.95 | 377.35 | $1.14 \times 10^{8}$ | $2.25 \times 10^{18}$ |

where $n_t$ is the total particle number-concentration.

## Results and Discussion

***Carbon-DM inks.***—*Experimental observation.*—As time progresses, collisions between carbon particles in the ink will lead to the formation of larger aggregates. The larger aggregate size will lead to a lower particle concentration at the top compared to the bottom of the colloidal system in consideration. This will lead to a phase separation of DM and carbon particles in the ink. The time required for the colloidal particles to separate from each of the studied DM was noted based on visual inspection. Figure 2 shows the effect of DM on carbon stability for the four cases. Based on visual inspection, ethyl acetate and methanol based inks became unstable (phase-separated) in under 2 minutes after their preparation, the IPA based ink was observed to be stable for more than 30 days and the ethanol based ink was found to be stable for around 8 to 12 days. Based on these observation, IPA was found to be a better DM for Vulcan carbon black.

*Model prediction.*—To analyze these observations, Equation 5 was used to determine the interaction energy between the particles, which was then used to determine the values of stability ratio, $W$, and rates of particle aggregation. Table II gives the calculated values of the stability ratio for particle diameter from 25 nm to 120 nm for the four DM. It can be seen that for all the DM, $W$ increases with particle size indicating that the rate of aggregation decreases as the aggregate size increases. $W$ was found to be a strong function of particle size for IPA
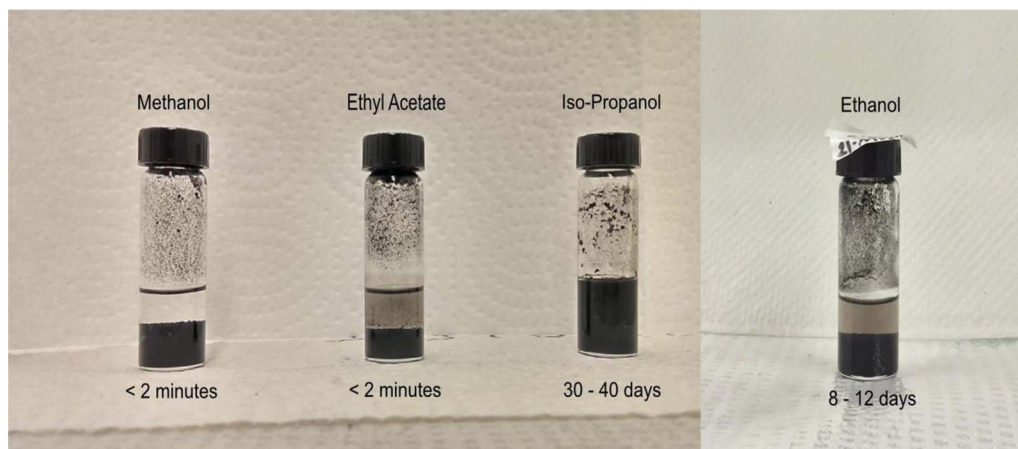


**Figure 2.** Effect of DM on carbon ink stability. Stability time for each DM is given below the image.
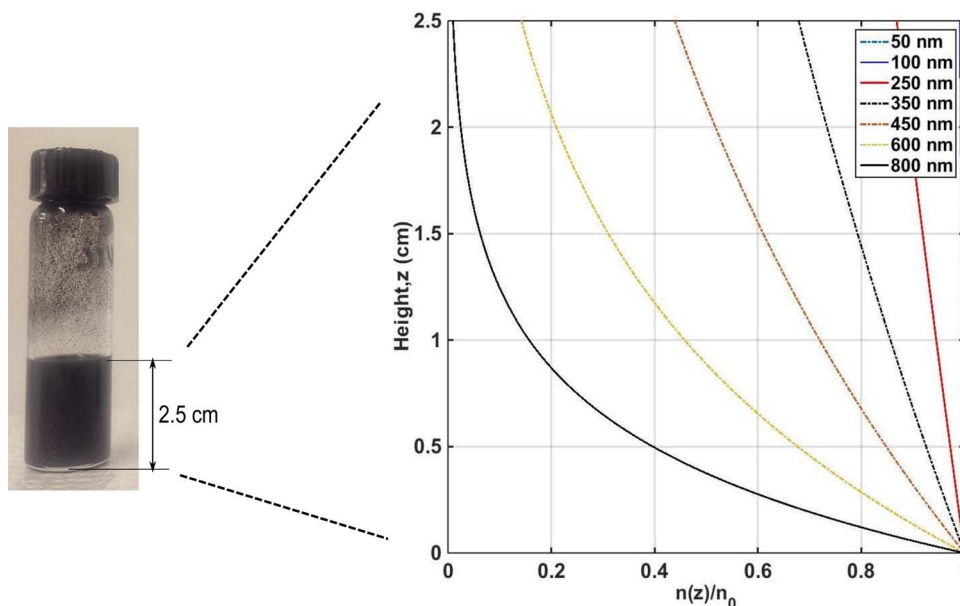
**Figure 3.** Number-density profiles of particles in IPA. Smaller particles appear to be well dispersed while sedimentation is more prominent for larger particles.

followed by ethanol, methanol and finally ethyl acetate. Lower values of $W$ for ethyl acetate and methanol indicate unstable dispersion as observed experimentally. The calculated values of $W$ for IPA and ethanol beyond 90 nm are in agreement with the definition of a stable dispersion, i.e., $W > 10^5$.[36] The stability ratio may therefore be a good qualitative indicator for determining whether a dispersion is stable or not.

Quantification of time for which the inks remain dispersed required calculating the time needed for the carbon particles to reach a threshold size beyond which they would settle toward the bottom of the glass vial. The threshold aggregate size was calculated based on the number-density profile using Equation 13. Figure 3 shows the particle distribution profile for different particle sizes from 50 nm to 800 nm in IPA. The height, $z$, plotted on the $y$-axis matched the height of the ink in the vial used for the experimental study. The $x$-axis shows fraction of the particle-concentration as a function of height, $z$. It can be seen from Figure 3 that for particle sizes of 50 and 100 nm, little or no variation in the density profile is observed for the entire colloidal system height. As the aggregate size increases further, concentration toward the top starts to drop indicating that diffusion is lagging behind sedimentation to maintain particle distribution throughout the medium. For an aggregate size of 450 nm, the particle concentration at the top is 44% of the total concentration and at 800 nm, the particle concentration at the top is close to 0%.

The threshold aggregate size beyond which the ink is considered as unstable based on visual inspection is subjective. It will depend on how uniform we want the particle distribution in the ink to be and the height of the colloidal system into consideration. For this case, the threshold size is considered to be 450 nm where the particle number concentration at the top of the vial is less than 50% of the total number of particles in the system.

Based on the calculated values of $W$, Equations 8 and 16 were used to plot a decay rate of the primary particles (normalized) with time considering polydispersed and monodispersed particle sizes respectively. Figure 4 shows the rate of change of primary particle concentration ($n_1$) to aggregates of 15 primary particles ($n_{15}$) normalized with the original particle concentration ($n_0$). Particle aggregates $> n_{15}$ will also be formed but have not been accounted for in Figure 4. Here, $n_1/n_0$ decreases exponentially giving rise to the formation of dimers, trimers and so on. Ethyl acetate and methanol based inks appear to be unstable compared to ethanol and IPA, based on a rapid drop in the particle concentration, whereas IPA based ink appears to be

the most stable. The normalized concentration of the particles ($n_t/n_0$) plotted with respect to time $t$ is shown in Figure 5 for monodispersed particles. Similar to Figure 4, the decay in particle concentration is seen to be delayed for the case of an IPA based ink as compared to others, as observed experimentally.

Considering an aggregate size of 450 nm (assumed threshold limit), the number of primary particles per aggregate is found to be 1889 based on Equation 14 and as a result, the ratio $n_t/n_0$ was calculated to be 0.00053. As highlighted in Figure 5, this corresponded to a time of 12.9 hours, 22.5 hours, 6.0 days and 162.8 days for ethyl acetate, methanol, ethanol and IPA, respectively. Table III shows a comparison of the experimentally observed and calculated stability times. It is possible that even after ultrasonic mixing, the original carbon aggregates could not be separated and that the original carbon particle size is of the order of 100 nm, therefore, the predicted stability time when the primary particle size is 100 nm instead of 25 nm is also given in Table III. In both cases, the calculated values largely over-predict the time until which the ink will remain dispersed, however the correct trends are observed. The difference appears to be higher when a larger primary particle size is considered, and is likely due to the relationship between the stability ratio and particle size as shown previously in Table II.

The quantitative discrepancy between the measured and calculated values of the stability time for the different DM may arise from the validity of the assumptions used in the calculations. For simplicity, the carbon particles and aggregates have been idealized using a diameter of 25 nm. This may not be an accurate representation since the nanoparticle aggregates may form complex structures, such as fractals or rod like structures, instead of spherical aggregates.[42–45] Including a more realistic particle morphology based on experimental observations may help to reduce the quantitative discrepancy and make the model more accurate in predicting the stability time. Attempts to include complex aggregate shapes could be implemented in order to improve the accuracy of the proposed simplistic model. Other forms of aggregation such as orthokinetic aggregation and differential sedimentation may influence the rates of aggregation in the later stages of the process. Further, multi-body interactions that might better track the aggregation rate have not been considered in this work.[46] In-spite of these differences, the experimental observations of ink stability can be qualitatively explained with the model. Given the primary particle size and its zeta potential in a DM, it is possible to predict the stability of the ink dispersion.
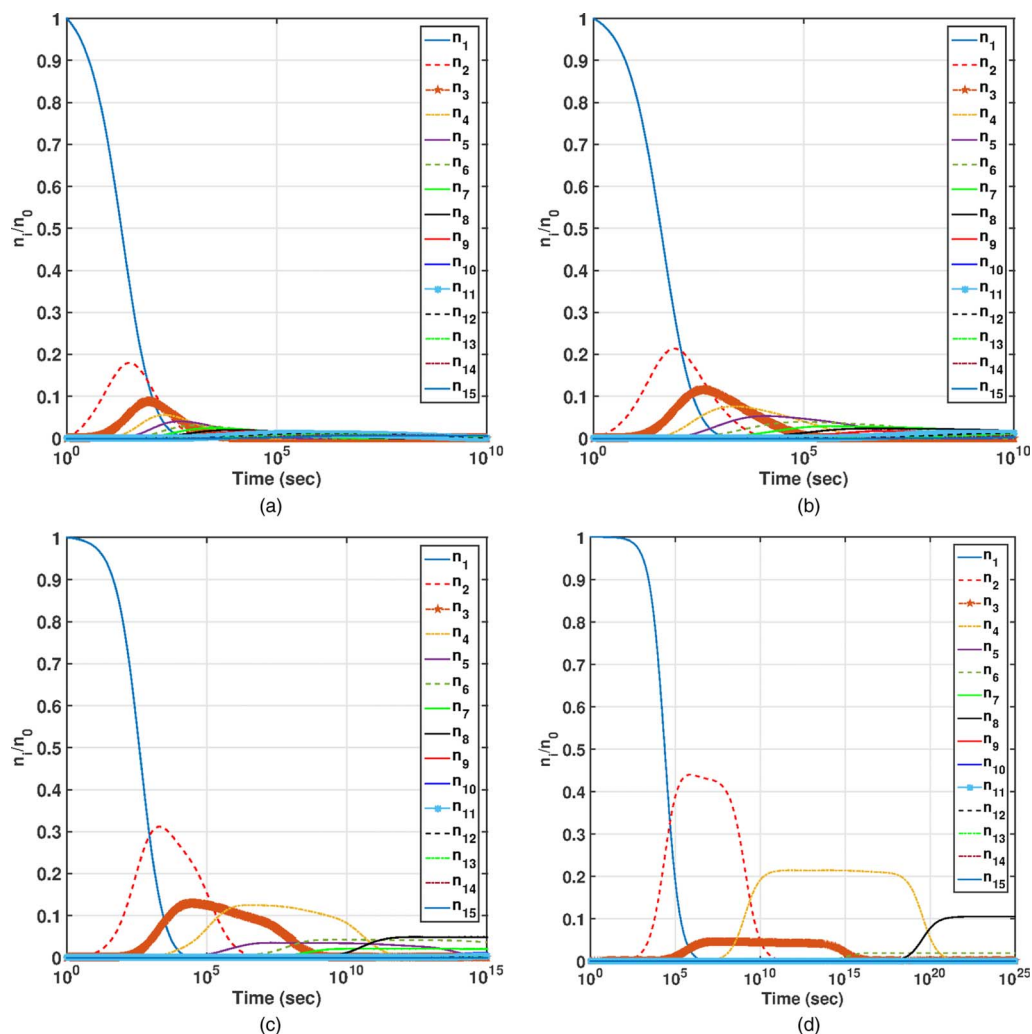
**Figure 4.** Rate of change of monomer units ($n_1$ to $n_{15}$) with time based on Equation 8 (a) ethyl acetate (b) methanol (c) ethanol and (d) IPA.
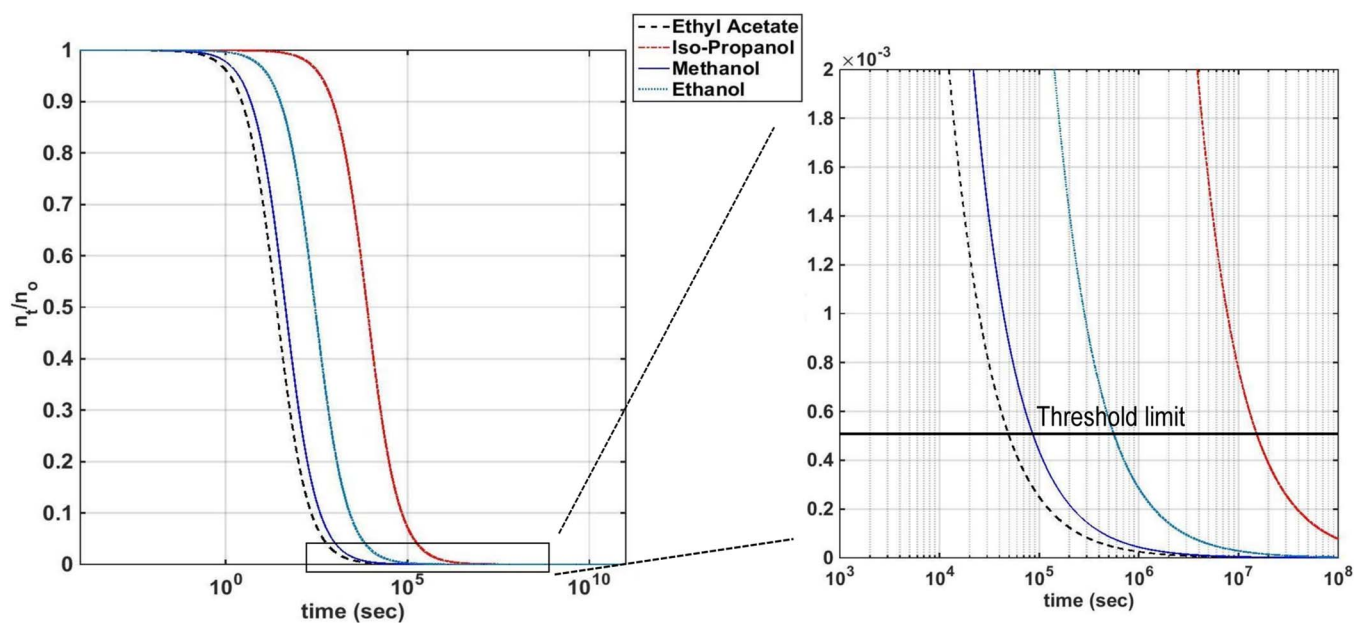


**Figure 5.** Rate of decay in particle concentration (normalized) with time based on Equation 16. Magnified image indicates the threshold limit when the particle size reaches 450 nm.

**Table III. Comparison of stability time for carbon dispersion in the respective DM based on visual inspections and model prediction.**

| DM | Experimental observation | Model prediction (25 nm) | Model prediction (100 nm) |
|---|---|---|---|
| Ethyl Acetate | < 2 minutes | 12.9 hours | 4.1 days |
| Methanol | < 2 minutes | 22.5 hours | 130.6 days |
| Ethanol | 8–12 days | 6.0 days | $5.3 \times 10^6$ days |
| Iso-propanol | 30–40 days | 162.8 days | $1.8 \times 10^{15}$ days |

***Effect of Nafion.***—Apart from facilitating protonic transport through the electrodes, addition of Nafion ionomer to the ink appears to also enhance the ink stability by providing an additional repulsive energy between the particles in the form of steric interaction. It was observed that carbon particles that may be unstable in a DM become stable after addition of Nafion. Quantification of the steric potential is complex because of its dependence on a number of parameters such as the type of DM, temperature, attachment mechanism and polymer concentration.[35] For the reasons above and due to the lack of quantitative literature data, the steric interaction potential was not implemented in the model. The effect of Nafion addition on the ink stability was however studied experimentally.

*Experimental observation.*—Experiments were performed to study the effect of Nafion by adding 30 wt% Nafion ionomer for each DM type and the ink stability was analyzed. The rate of change in particle size with time for Nafion loadings of 10 wt%, 30 wt% and 50 wt% was also carried out for the case of IPA based ink to see if the particle size was a function of the amount of ionomer added.
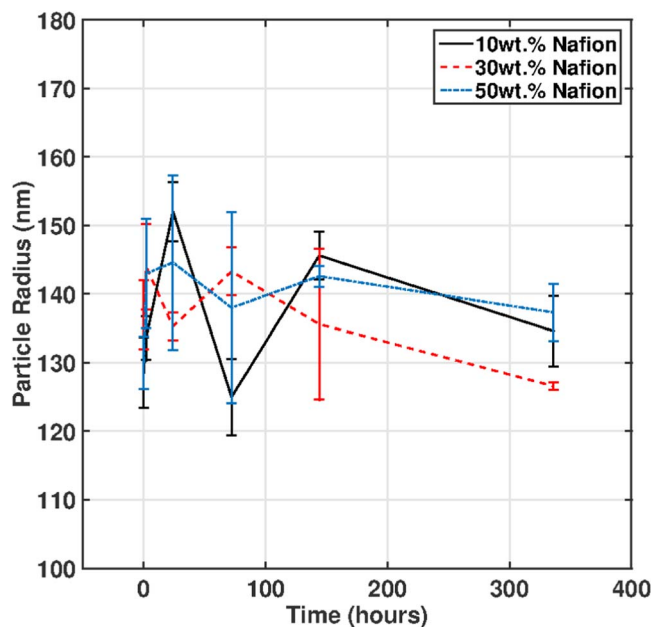
Addition of Nafion increased the ink stability time for the two DM cases that were unstable prior to the addition of Nafion viz., ethyl acetate and methanol. It also resulted in a reduced measured particle size for the IPA based ink. However, unlike the methanol based ink, DM containing ethyl acetate remained stable for only a few hours. Table IV shows the particle sizes using DLS before and after the addition of Nafion using a dilute ink solution and the ALV/CGS-3 goniometer system. Methanol and IPA based DM show a lower particle size compared to ethyl acetate based DM after ionomer was added.

Further, in order to determine whether the particle size was a function of the amount of Nafion being introduced in the ink, three inks with Nafion loadings of 10 wt%, 30 wt% and 50 wt% were prepared using IPA as the DM. The particle size for the prepared samples was measured using DLS with varying time intervals from 2 hours to 14 days. Figure 6 shows the average particle size measured for the three Nafion loading cases. No specific trend for particle size with time was observed. Even after 14 days, there was no increase in particle size for each of the three Nafion loading cases. Thus, even a small amount of ionomer added to the ink is sufficient to increase its stability for a prolonged period of time for the IPA based ink.

*Model prediction.*—Theoretical quantification of the stability time for DM with the ionomer is not possible since the steric term has not been accounted for in the model. However, an explanation based on the magnitude of Coulombic interaction for the experimental observation could be given. The zeta potential, which affects the magnitude of the Coulombic interaction between the particles, changes with ion



**Figure 6.** Effect of Nafion loading on particle size for carbon black in IPA based ink.

concentration.[42] It has been observed that addition of Nafion solution (mixture of water and volatile organic compounds) to the DM increases the $H^+$ ion concentration due to the presence of sulphonic acid groups in the ionomer. This will affect the surface potential of the particles.[42] A parametric study of surface potential was carried out for the four DM as shown in Figure 7. For a particle size of 30 nm, Figure 7a shows the effect of inter-particle distance ($h$) on the dimensionless interaction energy ($U/kT$) for the four DM. Based on this, the variation in the maximum interaction energy with surface potentials ranging from $-100$ mV to $+100$ mV is plotted in Figure 7b. Interaction energy was found to be a strong function of the surface potential for the case of IPA, ethanol and methanol compared to ethyl acetate. Thus, any change in ζ resulting from the addition of ionomer would cause a greater increase in the repulsive interaction energy for the case of IPA, ethanol and methanol as compared to ethyl acetate.

To generalize this observation, the effect of interaction energy on a range of dielectric constants from 0 to 100 and surface potentials ranging from $-100$ mV to $+100$ mV is plotted in Figure 8. The variation of interaction energy with the DM refractive index is found to be minimal. A higher value of interaction energy corresponded to a better DM in terms of ink stability, as it prevented aggregation of particles. It was seen that with increasing dielectric constant of the DM, the dependence of interaction energy on surface potential increases. Thus, varying the particle zeta potential either by functionalizing the carbon particles or changing the ionomer concentration may only be beneficial for higher dielectric constant DM such as methanol to improve the ink stability.

***Effect of ink dilution.***—Typically, DLS measurements require diluting the ink sample to reduce multiple-scattering and allow for a consistent data. Due to this restriction, the accuracy of this technique has been questioned for the case of measuring particle size of catalyst inks.[1] The most recent DLS instruments, e.g., NanoPlus 3, Micromeritics, allow a broad range of particle concentrations to be analyzed by tilting the sample and reducing the volume of sample the light needs to traverse. This instrument was used to study the effect the effect of dilution on particle size.

An ink sample consisting of 12.5 mg of Vulcan XC72 carbon black, 3.5 mL IPA and 0.32 mL 5 wt% Nafion solution (equivalent to approximately 50 wt% Nafion loading) was studied. Five particle concentrations were tested for their particle size, i.e., ink without
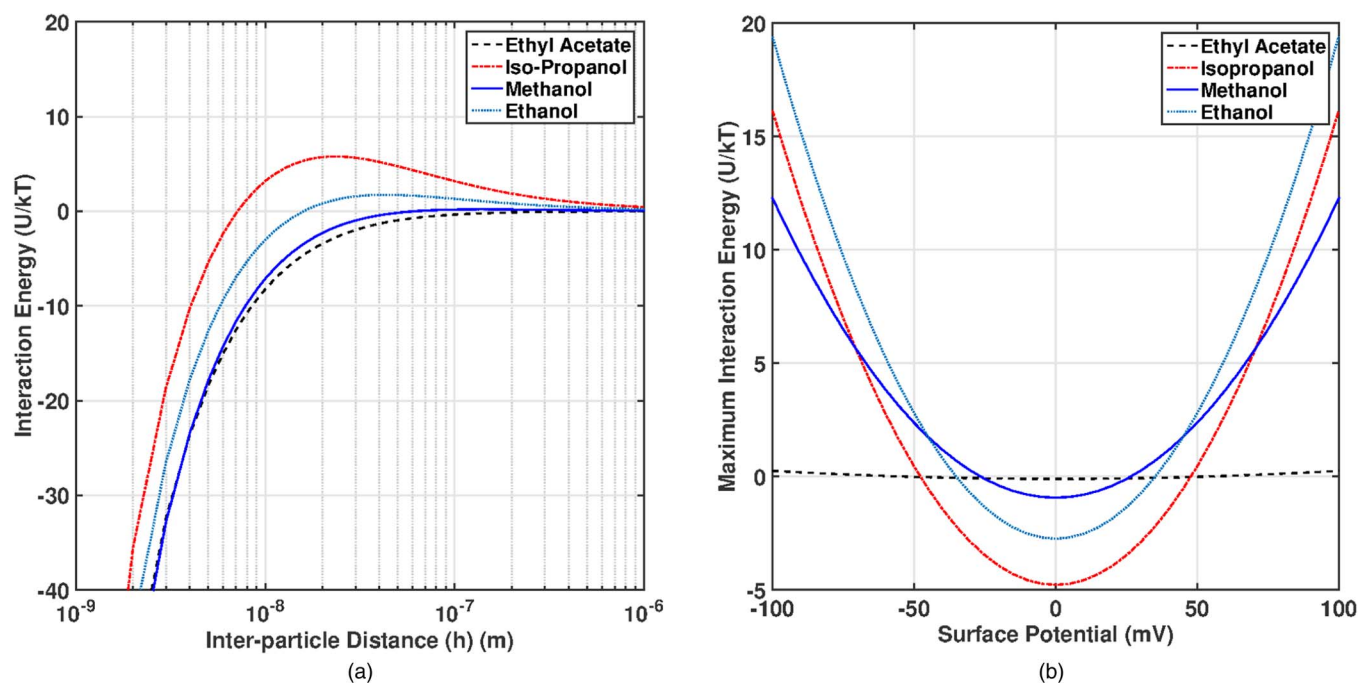
**Table IV. Average hydrodynamic diameter (nm) for carbon black dispersed in IPA, methanol and ethyl acetate with and without Nafion ionomer based on DLS.**

| IPA | | Methanol | | Ethyl Acetate | |
|---|---|---|---|---|---|
| Without Nafion | With Nafion | Without Nafion | With Nafion | Without Nafion | With Nafion |
| $804 \pm 60$ | $266 \pm 12$ | unstable | $274 \pm 10$ | unstable | $1022 \pm 298$ |

**Figure 7.** Model prediction for the effect of surface potential on interaction energy for the four DM for a particle size of 30 nm. (a) Variation of interaction energy with inter-particle distance (b) Variation of maximum interaction energy with surface potential. IPA, methanol and ethanol show a higher dependence on potential compared to ethyl acetate.

dilution, 1 mL ink in 1 mL IPA (1:1), 1 mL ink in 5 mL IPA (1:5), 1 mL ink in 10 mL IPA (1:10) and 1 mL ink in 100 mL IPA (1:100). The corresponding particle concentrations for these inks are given in Table V. The non-diluted ink is tested first, then diluted to the desired amount with IPA, mixed in an ultrasonic bath for at least 30 min, and finally tested in the DLS. Figure 9 shows the experimental data obtained from DLS for the different samples. The corresponding particle size and poly-dispersity (PD) index are given in Table V (standard deviation is based on eight measurements). These particle sizes differ from those reported in Table IV because, in this case, the cumulants diameter is reported instead of the hydrodynamic diameter.

**Table V. Effect of particle size and poly-dispersity index on particle concentration based on DLS in IPA.**

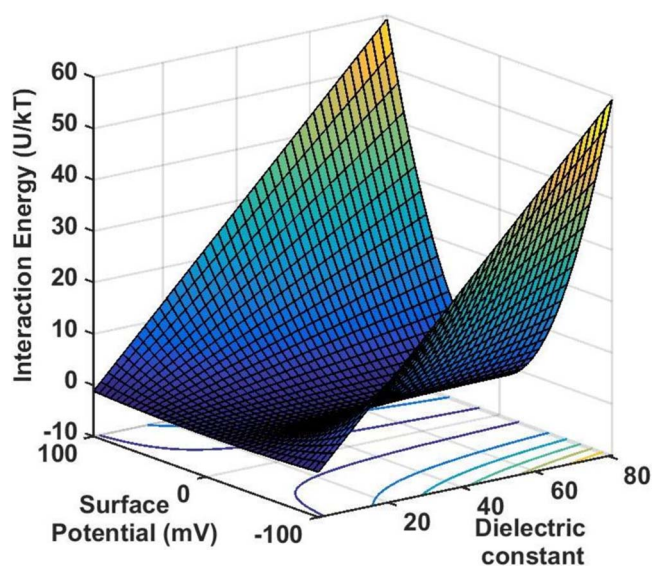| Ink sample | Particle volume concentration (%) | Average particle diameter (nm) | Poly-dispersity index |
|---|---|---|---|
| no dilution | 0.19 | $284.5 \pm 9.3$ | $0.167 \pm 0.019$ |
| 1:1 | 0.096 | $259.5 \pm 9.3$ | $0.148 \pm 0.026$ |
| 1:5 | 0.032 | $245.6 \pm 8.5$ | $0.123 \pm 0.016$ |
| 1:10 | 0.018 | $237.1 \pm 7.8$ | $0.098 \pm 0.033$ |
| 1:100 | $1.91 \times 10^{-3}$ | $233.1 \pm 5.3$ | $0.083 \pm 0.045$ |



**Figure 8.** Model prediction for the effect of varying surface potential and dielectric constants on interaction energy for an inter-particle distance of 50 nm and a DM refractive index of 1.37.
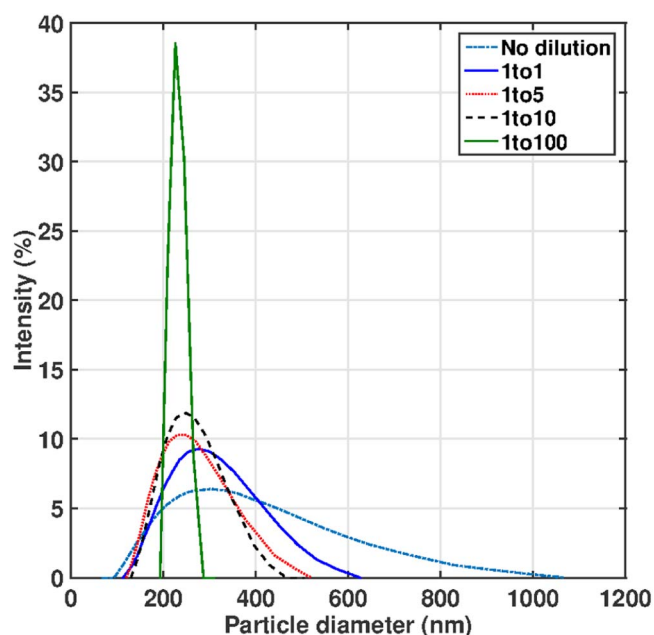


**Figure 9.** Effect of ink dilution on the carbon particle size in IPA based on DLS.

Table V shows that the particle size of the carbon ink decreases with increasing dilution. The change however is relatively small, with particle diameter decreasing from $284.5 \pm 9.3$ nm to $233.1 \pm 5.3$ nm, i.e., by less than 20%, as the solid content decreased from 0.19 vol.% to $1.91 \times 10^{-3}$ vol.%. The largest change in particle size occurs as the ink is diluted with 1 and 5 mL of IPA. Further dilution has a nearly insignificant effect on particle size. Therefore, particle size using diluted inks can be considered to provide reasonable results. The slight drop in particle size with dilution is because a lower particle concentration reduces the probability of inter-particle collisions that lead to formation of larger aggregates. Even though the average particle size is only slightly affected by dilution, Figure 9 and the PD index in Table V, which dropped from 0.167 for the ink without dilution to 0.083 for the 1:100 ink, indicate that dilution has an effect on the particle size distribution with diluted inks having a narrower range of particle sizes.

## Conclusions

The effect of dispersion media on the stability of carbon inks was studied for the case of four non-aqueous media: IPA, methanol, ethanol and ethyl acetate. The stability time for the different ink dispersions was estimated based on visual inspection. IPA was found to be the best dispersing agent for carbon. To understand the experimental observations and develop a methodology to optimize the DM selection, a semi-empirical model comprising van der Waals and Coulombic interactions was implemented to calculate the stability ratios and rates of aggregation. Using the theoretical model, the settling time for the four carbon inks was calculated using diffusion-limited aggregation kinetics and assuming a threshold aggregate size of 450 nm based on the sedimentation-diffusion equilibrium. Experimental observations and theoretical predictions were shown to agree qualitatively.

The addition of Nafion ionomer to carbon inks was studied experimentally. As expected from theory, the addition of Nafion helped to increase the ink stability and reduce the particle size. In the case of IPA, the addition of Nafion reduced the particle size from $804 \pm 60$ nm to $266 \pm 12$ nm. The increase in ink stability with Nafion addition was observed even at small Nafion loadings and independent of the amount of Nafion used. Further, the effect of Nafion is shown to be stronger for the case of dispersions with a higher dielectric constant where the interaction energy is a strong function of surface potential.

Finally, one of the main drawbacks of dynamic light scattering is that diluted inks need to be used. To study the effect of dilution in the particle size, a recent dynamic light scattering apparatus was used to measure particle size with and without dilution. Results show that increasing dilution decreases particle size, but the effect of dilution is relatively small, i.e., less than 20% for the ink under study.

## Acknowledgments

## References

1. S. Holdcroft, Fuel cell catalyst layers: a polymer science perspective, *Chemistry of Materials*, **26**(1), 381 (2013).
2. J. Wee, K. Lee, and S. Kim, Fabrication methods for low-pt-loading electrocatalysts in proton exchange membrane fuel cell systems, *Journal of Power Sources*, **165**(2), 667 (2007).
3. M. Saha, M. Tam, V. Berejnov, D. Susac, S. McDermid, A. P. Hitchcock, and J. Stumper, Characterization and performance of catalyst layers prepared by inkjet printing technology, *ECS Transactions*, **58**(1), 797 (2013).
4. S. Shukla, K. Domican, K. Karan, S. Bhattacharjee, and M. Secanell, Analysis of low platinum loading thin polymer electrolyte fuel cell electrodes prepared by inkjet printing, *Electrochimica Acta*, **156**, 289 (2015).
5. S. Shukla, D. Stanier, M. S. Saha, J. Stumper, and M. Secanell, Analysis of inkjet printed pefc electrodes with varying platinum loading, *Journal of The Electrochemical Society*, **163**(7), F677 (2016).
6. S. Shukla, K. Domican, and M. Secanell, Effect of electrode patterning on pem fuel cell performance using ink-jet printing method, *ECS Transactions*, **64**(3), 341 (2014).
7. Z. Xie, X. Zhao, M. Adachi, Z. Shi, T. Mashio, A. Ohma, K. Shinohara, S. Holdcroft, and T. Navessin, Fuel cell cathode catalyst layers from green catalyst inks, *Energy & Environmental Science*, **1**(1), 184 (2008).
8. B. Millington, V. Whipple, and B. Pollet, A novel method for preparing proton exchange membrane fuel cell electrodes by the ultrasonic-spray technique, *Journal of Power Sources*, **196**(20), 8500 (2011).
9. Shantanu T. Shukla, *Experimental analysis of inkjet printed polymer electrolyte fuel cell electrodes*. PhD thesis, University of Alberta, 2016.
10. L. Sun, H. Zhang, J. Ilavsky, Z. Li, and J. Xie, Investigation of solvent effects on the dispersion of carbon agglomerates and nafion ionomer particles in catalyst inks using ultra small angle X-ray scattering and cryo-tem, *ECS Transactions*, **50**(2), 1461 (2013).
11. S. Shin, J. Lee, H. Ha, S. Hong, H. Chun, and I. Oh, Effect of the catalytic ink preparation method on the performance of polymer electrolyte membrane fuel cells, *Journal of power sources*, **106**(1), 146 (2002).
12. M. Moore, P. Wardlaw, P. Dobson, J. Boisvert, A. Putz, R. Spiteri, and M. Secanell, Understanding the effect of kinetic and mass transport processes in cathode agglomerates, *Journal of the Electrochemical Society*, **161**(8), E3125 (2014).
13. M. Eikerling, A. Kornyshev, and A. Kucernak, Water in polymer electrolyte fuel cells: Friend or foe?, *Physics today*, **59**(10), 38 (2006).
14. T. Greszler, D. Caulk, and P. Sinha, The impact of platinum loading on oxygen transport resistance, *Journal of The Electrochemical Society*, **159**(12), F831 (2012).
15. A. Weber and A. Kusoglu, Unexplained transport resistances for low-loaded fuel-cell catalyst layers, *J. Mater. Chem. A*, **2**, 17207 (2014).
16. L. Hao, K. Moriyama, W. Gu, and C. Wang, Modeling and experimental validation of pt loading and electrode composition effects in pem fuel cells, *Journal of The Electrochemical Society*, **162**(8), F854 (2015).
17. W. Yoon and A. Z. Weber, Modeling low-platinum-loading effects in fuel-cell catalyst layers, *Journal of The Electrochemical Society*, **158**(8), B1007 (2011).
18. C. Welch, A. Labouriau, R. Hjelm, B. Orler, C. Johnston, and Yu S. Kim, Nafion in dilute solvent systems: Dispersion or solution?, *ACS Macro Letters*, **1**(12), 1403 (2012).
19. G. Gebel and B. Loppinet, Colloidal structure of ionomer solutions in polar solvents, *Journal of molecular structure*, **383**(1-3), 43 (1996).
20. P. Aldebert, B. Dreyfus, and M. Pineri, Small-angle neutron scattering of perfluorosulfonated ionomers in solution, *Macromolecules*, **19**(10), 2651 (1986).
21. M. Uchida, Y. Aoyama, N. Eda, and A. Ohta, New preparation method for polymer-electrolyte fuel cells, *Journal of The Electrochemical Society*, **142**(2), 463 (1995).
22. M. Uchida, Y. Fukuoka, Y. Sugawara, H. Ohara, and A. Ohta, Improved preparation process of very-low-platinum-loading electrodes for polymer electrolyte fuel cells, *Journal of The Electrochemical Society*, **145**(11), 3708 (1998).
23. M. Chisaka and H. Daiguji, Effect of organic solvents on catalyst layer structure in polymer electrolyte membrane fuel cells, *Journal of The Electrochemical Society*, **156**(1), B22 (2009).
24. D. Huang, P. Yu, F. Liu, S. Huang, K. Hsueh, Y. Chen, C. Wu, W. Chang, and F. Tsau, Effect of dispersion solvent in catalyst ink on proton exchange membrane fuel cell performance, *Int. J. Electrochem. Sci*, **6**, 2551 (2011).
25. B. Millington, S. Du, and B. Pollet, The effect of materials on proton exchange membrane fuel cell electrode performance, *Journal of Power Sources*, **196**(21), 9013 (2011).
26. K. Malek, M. Eikerling, Q. Wang, T. Navessin, and Z. Liu, Self-organization in catalyst layers of polymer electrolyte fuel cells, *The Journal of Physical Chemistry C*, **111**(36), 13627 (2007).
27. Y. Xiao, M. Dou, J. Yuan, M. Hou, W. Song, and B. Sundén, Fabrication process simulation of a pem fuel cell catalyst layer and its microscopic structure characteristics, *Journal of The Electrochemical Society*, **159**(3), B308 (2012).
28. R. Xu, C. Wu, and H. Xu, Particle size and zeta potential of carbon black in liquid media, *Carbon*, **45**(14), 2806 (2007).
29. S. Shukla, S. Bhattacharjee, and M. Secanell, Rationalizing catalyst inks for pemfc electrodes based on colloidal interactions, *ECS Transactions*, **58**(1), 1409 (2013).
30. J. Larruquert, Rodríguez. de M, J. Méndez, P. Martin, and A. Bendavid, High reflectance ta-c coatings in the extreme ultraviolet, *Optics express*, **21**(23), 27537 (2013).
31. M. Polyanskiy, Refractive index database, 2014. https://refractiveindex.info/?shelf=main&book=C&page=Larruquert. Accessed: February 15, 2017.
32. W. Anderson, D. Kozak, V. Coleman, A. Jämting, and M. Trau, A comparative study of submicron particle sizing platforms: Accuracy, precision and resolution analysis of polydisperse particle size distributions, *Journal of colloid and interface science*, **405**, 322 (2013).
33. M. Elimelech, X. Jia, J. Gregory, and R. Williams, *Particle deposition & aggregation: measurement, modeling and simulation*, Butterworth-Heinemann, 1998.
34. D. Santiago, G. Rodríguez-Calero, H. Rivera, D. Tryk, M. Scibioh, and C. Cabrera, Platinum electrodeposition at high surface area carbon vulcan-xc-72r material using a rotating disk-slurry electrode technique, *Journal of The Electrochemical Society*, **157**(12), F189 (2010).

35. J. Israelachvili, *Intermolecular and surface forces: revised third edition*. Academic press, 2011.
36. I. Morrison, Criterion for electrostatic stability of dispersions at low ionic strength, *Langmuir*, **7**(9), 1920 (1991).
37. J. Masliyah and S. Bhattacharjee, *Electrokinetic and Colloid Transport Phenomena*. Wiley Online Library, 2006.
38. J. Berg, *Introduction to Interfaces and Colloids*. World Scientific Publishing Company Incorporated, 2009.
39. A. Marmur, A kinetic theory approach to primary and secondary minimum coagulations and their combination, *Journal of Colloid and Interface Science*, **72**(1), 41 (1979).
40. Micromeritics. http://www.micromeritics.com/Repository/Files/apnote94.pdf. Accessed: March 17, 2017.
41. T. Soboleva, X. Zhao, K. Malek, Z. Xie, T. Navessin, and S. Holdcroft, On the micro-, meso-, and macroporous structures of polymer electrolyte membrane fuel cell catalyst layers, *ACS applied materials & interfaces*, **2**(2), 375 (2010).
42. B. Viswanath, S. Patra, N. Munichandraiah, and N. Ravishankar, Nanoporous pt with high surface area by reaction-limited aggregation of nanoparticles, *Langmuir*, **25**(5), 3115 (2009).
43. S. Takahashi, J. Shimanuki, T. Mashio, A. Ohma, H. Tohma, A. Ishihara, Y. Ito, Y. Nishino, and A. Miyazawa, Observation of ionomer in catalyst ink of polymer electrolyte fuel cell using cryogenic transmission electron microscopy, *Electrochimica Acta*, **224**, 178 (2017).
44. M. Shibayama, T. Matsunaga, T. Kusano, K. Amemiya, N. Kobayashi, and T. Yoshida, Sans studies on catalyst ink of fuel cell, *Journal of Applied Polymer Science*, **131**(3), (2014).
45. F. Xu, H. Zhang, J. Ilavsky, L. Stanciu, D. Ho, M. Justice, H. Petrache, and J. Xie, Investigation of a catalyst ink dispersion using both ultra-small-angle X-ray scattering and cryogenic tem, *Langmuir*, **26**(24), 19199 (2010).
46. G. Kwon, Y. Won, and B. Yoon, Electrical double-layer interactions of regular arrays of spheres, *Journal of colloid and interface science*, **205**(2), 423 (1998).